JOURNAL OF CATALYSIS 97, 456–468 (1986)

Oscillations during CO Oxidation over Supported Metal Catalysts

III. Mathematical Modeling of the Observed Phenomena

DAVID T. LYNCH,[1] GERHARD EMIG,[2] AND SIEGHARD E. WANKE

Department of Chemical Engineering, University of Alberta, Edmonton, Alberta T6G 2G6, Canada

Received April 24, 1985; revised September 3, 1985

A detailed mathematical model has been developed for the prediction of oscillatory behavior during CO oxidation on supported metal catalysts. This model is based on the hypothesis that the adsorption of CO causes reversible changes in the surface structure of the metal. The changes in the surface phase result in changes in the rate of O_2 adsorption. A detailed comparison has been made between the predictions of this model and experimental observations. Excellent model–experimental agreement has been obtained for a wide range of operating parameters. During an oscillatory cycle the model predicts that the system alternates between a region in which oxygen adsorption is rate controlling, and one in which there is a sensitive balance between the rates of the adsorption and the reaction steps. © 1986 Academic Press, Inc.

INTRODUCTION

Self-sustained oscillations are frequently observed during the heterogeneously catalyzed oxidation of carbon monoxide on noble metals. In an earlier study (*1*), the effects of reactor operating conditions on oscillatory behavior were investigated in detail. The operating conditions which were examined included reactor recycle ratio, gas phase temperature, feed composition, feed flow rate, and reactor pressure. These data can be used to validate mathematical models which are proposed to describe oscillatory behavior during CO oxidation.

In the last decade numerous mathematical models have been developed in attempts to explain oscillatory behavior for CO oxidation on supported metal catalysts. These models have been based on a variety of hypotheses, namely; activation energy dependence on the surface coverage (*2, 3*); reaction competition between linear and bridged forms of adsorbed CO (*4*); occurrence of physical processes such as the variation of the catalyst surface temperature (*5–8*); adsorption on inert (*9*) or coreacting (*10*), species which block catalytic sites; nonlinearities in the reaction mechanism due to the dissociative adsorption of oxygen (*11*); and oxidation/reduction of the catalyst surface (*12*). All of the models based on these hypotheses can predict the occurrence of self-sustained oscillatory behavior. However, quantitative comparisons (shape, frequency, and amplitude) of predicted and experimentally observed oscillations as a function of operating parameters have only been made in a few studies (*7, 12*).

In a recent experimental study (*13*), it has been proposed that oscillatory behavior could be caused by variations in the oxygen sticking probability due to the adsorbate-induced phase change of the catalyst surface. In this study we incorporate this new hypothesis into a mathematical model for a previously described experimental system (*1, 14*). The steady-state and dynamic behavior predicted by this model are described in detail, and a comprehensive comparison is made between the model

[1] To whom correspondence should be addressed.

[2] Present address: Institut für Technische Chemie I, Universität Erlangen-Nürnberg, Egerlandstrasse 3, 8520 Erlangen, FRG.

0021-9517/86 $3.00

predictions and the experimental observations reported previously (*1*).

REACTION MECHANISM

In this study it is assumed that CO oxidation proceeds by a Langmuir–Hinshelwood mechanism with the modification that the rate of O_2 adsorption is a strong function of CO surface coverage. This strong dependence of the O_2 sticking probability on CO coverage is due to the postulated changes in metal surface phases as a function of CO coverages. Such changes in surface phases have been well documented in single crystal studies (*13*, *15–18*).

The mechanism and energetics of the CO adsorption-induced transformation of the Pt(100) surface from a (5 × 20) to a (1 × 1) phase have been examined in detail (*15*, *16*). In these, and other (*17*, *18*), studies it has been shown that the Pt(100) surface is stable in a (5 × 20) phase when clean, but that this converts into a (1 × 1) phase when the fractional surface coverage of adsorbed CO, θ_{CO}, exceeds some critical value, $(\theta_{CO})_H$. If the CO surface coverage subsequently drops below another critical value, $(\theta_{CO})_L$, then the (1 × 1) phase converts back into the (5 × 20) phase. The experimental observation that $(\theta_{CO})_H$ and $(\theta_{CO})_L$ differ in value has been attributed to a nucleation process (*15*). This surface phase change can potentially cause oscillatory behavior to occur due to a difference in oxygen sticking probabilities on the two surface phases. It has been reported (*19*) that the oxygen sticking probability for the (1 × 1) phase can be several orders of magnitude greater than that for the (5 × 20) phase.

In the model presented in this paper, it is postulated that variations in CO coverage cause surface phase transformations (with concomitant changes in the O_2 sticking probability) in supported metal catalysts. The previously cited results obtained with single crystals justifies this postulate. The model does not require that all the metal surface experience phase changes; only part of the metal surface has to undergo these changes. However, phase changes are assumed to occur simultaneously on all crystallites, with the coupling among crystallites probably being via the gas phase concentration. The changes in surface phase and O_2 sticking probability are assumed to occur with the hysteresis effect shown in Fig. 1. The key assumption inherent in Fig. 1 is that surface phase 1 switches instantly to surface phase 2 when θ_{CO} becomes greater than $(\theta_{CO})_H$, or vice versa when θ_{CO} drops below $(\theta_{CO})_L$. Obviously this is a simplification of the actual behavior of the system since the phase transformation process will require a finite amount of

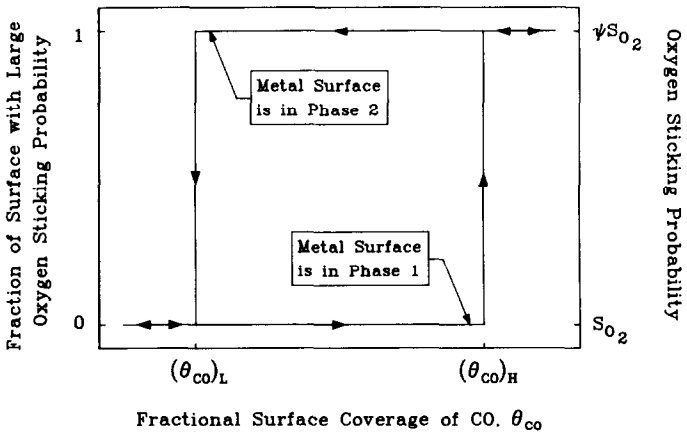

FIG. 1. Effect of CO coverage on the surface phase transformation.

time. However, the time required for the phase transformation has been observed to be 8 s or less (16) which is negligible when compared to the period of a typical oscillation which is ≥5 min (*1, 14*).

Thus, when the overall reaction is described in terms of elementary steps it is necessary to include alternate steps for oxygen adsorption. Incorporation of this phenomenon into the Langmuir–Hinshelwood mechanism yields the following mechanism.

$$CO(g) + M \underset{k_{-1}}{\overset{k_1}{\rightleftharpoons}} CO\text{-}M \quad (1)$$

$$O_2(g) + 2M_1 \xrightarrow{k_{2,1}} 2O\text{-}M \quad (2A)$$

$$O_2(g) + 2M_2 \xrightarrow{k_{2,2}} 2O\text{-}M \quad (2B)$$

$$CO\text{-}M + O\text{-}M \xrightarrow{k_3} CO_2(g) + 2M \quad (3)$$

$$CO_2(g) + S \underset{k_{-4}}{\overset{k_4}{\rightleftharpoons}} CO_2\text{-}S \quad (4)$$

In this mechanism, M represents a metal catalyst site, and S represents a support (γ-Al_2O_3) site for CO_2 adsorption/desorption. Only one of the two steps, (2A) or (2B), is operative at a given time depending on whether the metal catalyst surface is in phase 1 (M_1) or 2 (M_2). The appropriate step to use at a given time is fixed by the fractional surface coverage of CO as shown in Fig. 1. In the proposed mechanism, CO adsorption on the catalyst is not affected by the type of surface phase since it has been observed that the sticking probability of CO on (100) surfaces is not a strong function of the surface phase (*16*). It is also assumed that the surface reaction rate constant is not a function of the phase of the catalyst surface. The adsorption/desorption of CO_2 on/from the support material has been included because supports such as γ-Al_2O_3 exhibit a large capacity for CO_2 adsorption. It is important to note that support adsorption/desorption of CO_2 does not affect the catalytic production of the CO_2, but it does affect the dynamics of the gas-phase CO_2 concentrations.

MATHEMATICAL MODEL

The previously described (*14*) experimental reactor can be modelled as an isothermal CSTR due to the high recycle ratios which were employed. In the absence of mass transfer limitations, mass balances on the various gas and surface phase species produce the following six ordinary differential equations.

$$\frac{dX}{d\tau} = 1 - Q_n X - K_1 X(1 - \theta_{CO} - \theta_O) + K_{-1}\theta_{CO} \quad (5)$$

$$\frac{dY}{d\tau} = 1 - Q_n Y - K_2 Y(1 - \theta_{CO} - \theta_O)^2 \quad (6)$$

$$\frac{dZ}{d\tau} = -Q_n Z + K_3\theta_{CO}\theta_O - K_4 Z(1 - \phi_{CO_2}) + K_{-4}\phi_{CO_2} \quad (7)$$

$$\frac{d\theta_{CO}}{d\tau} = \alpha_m\{K_1 X(1 - \theta_{CO} - \theta_O) - K_{-1}\theta_{CO} - K_3\theta_{CO}\theta_O\} \quad (8)$$

$$\frac{d\theta_O}{d\tau} = \alpha_m\{(2F_{O_2}/F_{CO})K_2 Y(1 - \theta_{CO} - \theta_O)^2 - K_3\theta_{CO}\theta_O\} \quad (9)$$

$$\frac{d\phi_{CO_2}}{d\tau} = \alpha_s\{K_4 Z(1 - \phi_{CO_2}) - K_{-4}\phi_{CO_2}\} \quad (10)$$

where

$$Q_n = 1 - F_{CO}\{K_1 X(1 - \theta_{CO} - \theta_{CO}) - K_{-1}\theta_{CO}\} - F_{O_2}K_2 Y(1 - \theta_{CO} - \theta_O)^2 + F_{CO}K_3\theta_{CO}\theta_O - F_{CO}\{K_4 Z(1 - \phi_{CO_2}) - K_{-4}\phi_{CO_2}\}. \quad (11)$$

These equations have been written in dimensionless form, and the symbols are defined in the Appendix. The dimensionless parameters in the differential equations have been determined from the operating characteristics and physical dimensions of the reactor system, and from the rate constants for the elementary reaction steps. These parameters are as follows:

$$K_1 = 6.87\, a_m S_{CO}\sqrt{T}/Q_0 \quad (12)$$

$$K_{-1} = a_m L_m k_{-1} \exp(-E_{-1}/RT)/Q_0[CO]_0 \quad (13)$$

$$K_2 = 6.43\, a_m \psi S_{O_2}\sqrt{T}/Q_0 \quad (14)$$

$$K_3 = a_m L_m^2 k_3 \exp(-E_3/RT)/Q_0[CO]_0 \quad (15)$$

$$K_4 = 5.48\, a_s S_{CO_2}\sqrt{T}/Q_0 \quad (16)$$

$$K_{-4} = a_s L_s k_{-4} \exp(-E_{-4}/RT)/Q_0[CO]_0 \quad (17)$$

$$\alpha_m = V[CO]_0/a_m L_m \quad (18)$$

$$\alpha_s = V[CO]_0/a_s L_s \quad (19)$$

where the adsorption steps have been described using sticking probabilities and kinetic theory, and all activated steps follow the Arrhenius form. A parameter of particular importance in the definition of K_2 is ψ. When the surface of the catalyst is in phase 1, the parameter ψ has the value unity, and when the surface is in phase 2, ψ has a value greater than unity, i.e., ψ accounts for the dependence of the O_2 sticking probability on the state of the catalyst surface. As will be seen in the following sections, ψ is a key parameter in the proposed model.

STEADY-STATE BEHAVIOR OF THE MODEL

The first step which should always be performed when validating a model for oscillatory behavior is to examine the steady-state behavior predicted by the model. If the trends in the predicted steady-state behavior are not in agreement with experimental observations then the model should be immediately rejected even if oscillatory behavior can be predicted. Presented in Fig. 2 is a summary of the effects of reactor operating parameters on the experimentally observed transitions between oscillatory and steady-state behavior. Figure 2 has been constructed using data from Figs. 3, 5, and 6 of Ref. (*1*), as well as additional data that were not included in Ref. (*1*).

From Fig. 2a it is seen that increasing the percentage CO in the reactor feed results in the system passing from a stable high conversion steady state to a region of oscillatory behavior. Further increases in the feed CO move the system from the region of oscillations to a region of medium-to-low conversion steady states. It is also seen from Figs. 2b and c that increasing the total molar flow rate, or decreasing the bulk temperature, have effects similar to that described for increasing the percentage CO in the reactor feed. The model, which is proposed as a description of oscillatory behavior, should first be tested against the steady-state trends shown in Fig. 2.

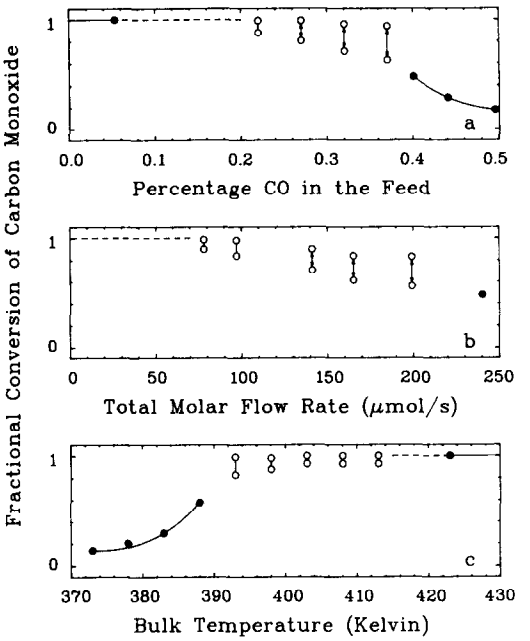

FIG. 2. Experimental effects of operating conditions.

The steady-state CO conversion behavior of the proposed model can be readily determined from the set of algebraic equations which result from setting the left-hand sides of Eqs. (5), (6), (8), and (9) equal to zero. It is not necessary to utilize Eqs. (7) and (10) since Z and ϕ_{CO_2} do not affect the steady-state reaction behavior. The steady-state behavior for a particular set of parameters (values given in the Appendix) is shown in Fig. 3; only the value of ψ is varied for the different plots in Fig. 3. The steady-state conversion of CO depends on θ_{CO} which determines the O_2 sticking proba-

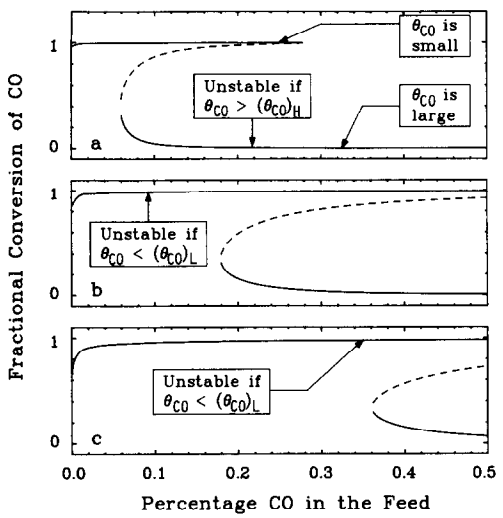

FIG. 3. Predicted steady-state behavior: (a) $\psi = 1$, (b) $\psi = 20$, (c) $\psi = 150$.

bility, i.e., ψ. The sequence of events leading to the steady-state predictions of the model is outlined below.

For an initially clean surface ψ is equal to unity (metal surface in phase 1) and the steady-state behavior for this case is shown in Fig. 3a. The value of ψ will remain at unity as long as θ_{CO} does not exceed $(\theta_{CO})_H$ (lower branch in Fig. 1). For the operating parameters used to obtain Fig. 3, θ_{CO} is very small as long as the system operates at a high CO conversion steady state, i.e., for CO in the feed <0.28%. For CO compositions of the feed ≥0.28%, the model predicts for $\psi = 1$ that the system will operate on the low conversion branch of Fig. 3a. However, θ_{CO} is very large (near unity) when operating at a low conversion steady state, and if θ_{CO} exceeds $(\theta_{CO})_H$ the transition from phase 1 to phase 2 occurs. It has been reported that $(\theta_{CO})_H$ can be as low as 0.5 (*15*). When the phase 1 to phase 2 transition occurs, ψ becomes greater than unity and the behavior shown in Fig. 3a no longer applies.

Shown in Figs. 3b and c are rate curves for $\psi = 20$ and $\psi = 150$, respectively. For the case of $\psi = 20$ and CO composition of the feed ≥0.28%, the reactor will operate at the low conversion steady state because the system is in the upper right region of Fig. 1 where phase 2 is stable. However, phase 2 is not stable for the high conversion state because θ_{CO} drops below $(\theta_{CO})_L$ which is ≤0.3 (*16*), and then the phase 2 to phase 1 transition occurs (see Fig. 1). Thus the reactor steady-state behavior is given by the high conversion branch in Fig. 3a ($\psi = 1$), and the low conversion branch in Fig. 3b or c ($\psi > 1$). If these two branches overlap as in Figs. 3a and b (between about 0.18 and 0.28% CO) then the reactor will exhibit multiple steady-state behavior in the overlap region.

However, if ψ is sufficiently large that the high and low conversion branches do not overlap, such as with Figs. 3a and c, then the reactor will not have any stable steady states in the gap region (between about 0.28 and 0.36% CO). This is because phase 2 for $\psi = 150$ only has a unique high conversion state for these CO feed concentrations, but phase 2 is unstable at these CO concentrations because θ_{CO} will be less than $(\theta_{CO})_L$. If the phase 2 to phase 1 transition occurs, then $\psi = 1$ and the system possesses only a unique low conversion state. However, this state is also unstable because θ_{CO} will be larger than $(\theta_{CO})_H$ at the low conversion conditions; hence, the phase 1 to phase 2 transition will occur. Thus the system will oscillate continuously between these two states.

In summary, for CO compositions of the feed <0.28% the system will operate on the stable high conversion branch shown in Fig. 3a, and for CO > 0.36% the system will operate on the stable low conversion branch shown in Fig. 3c. In the gap region (CO composition between 0.28 and 0.36%), self-sustained oscillations will occur if $\theta_{CO} > (\theta_{CO})_H$ when $\psi = 1$, and if $\theta_{CO} < (\theta_{CO})_L$ when $\psi = 150$. The overall system behavior is summarized in Fig. 4a.

A comparison of Figs. 4a and 2a shows that the trends in the predicted behavior are in excellent agreement with the experimental observations. Figures similar to Fig. 3 have been constructed using total molar flow rate and bulk temperature as the oper-

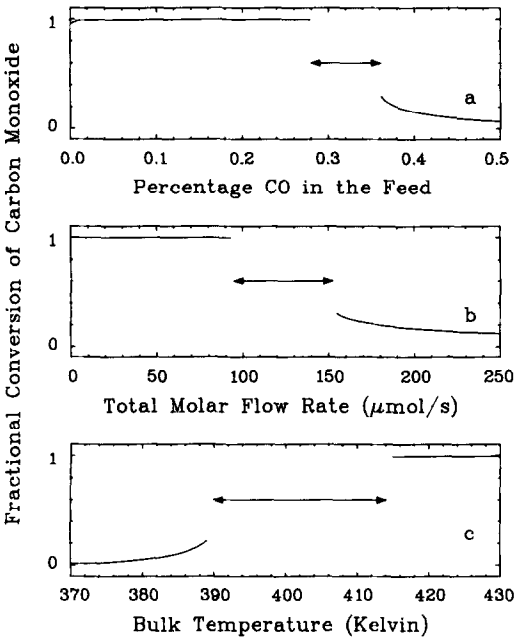

FIG. 4. Predicted effects of operating conditions (↔ indicates potential region of oscillations).

ating parameters of interest. These model predictions are summarized in Figs. 4b and c. A comparison of the corresponding parts of Figs. 4 and 2 shows that for all three of the operating parameters there is agreement between the model predictions and the experimental observations with respect to the passage from a low conversion steady state, to a region of oscillations, and then to a high conversion steady state when a particular operating parameter is varied. An exact determination of the bifurcation points for the transitions between steady-state and oscillatory behavior was not performed in the experimental study (*1*). Thus, it is not intended that the predicted and experimental oscillatory regions should match exactly since the exact widths of the experimental regions are not known. By an appropriate choice of the model parameters it is possible to place the predicted bifurcation points at essentially any location.

It is important to note that the same set of dimensional model parameters was used in all three parts of Fig. 4. These parameters, the values of which are all listed in the Appendix, were also held constant when determining the predicted dynamic behavior as reported in the following section. Thus, for the sake of consistency, all steady-state and dynamic predictions reported in this study have been based on a single set of model parameters. However, the dimensionless groupings are not constant, since from Eqs. (12) to (17) they are seen to be functions of the system operating conditions (T, Q_0, F_{CO}, etc.).

DYNAMIC BEHAVIOR OF THE MODEL

The predicted dynamic behavior was determined by integrating Eqs. (5) to (10). A set of integrations giving the reactor exit CO_2 concentrations (in terms of conversion) versus time are shown in Fig. 5 for various values of the CO concentration in the reactor feed (all other parameters are constant). For consistency with the experimental data, the feed CO was assumed to be from an 11% CO in nitrogen mixture, with the balance of the feed composed of oxygen. All integrations were performed using a Runge–Kutta–Fehlberg fourth/fifth-order integration algorithm (*20*) with error estimation and automatic step size adjustment. The initial conditions at the beginning of an integration were always $X = Y = Z = 0$ and $\theta_{CO} = \theta_O = \phi_{CO_2} = 0$. Since this set of initial conditions corresponds to an initially clean surface, a value of $\psi = 1$ was always used at the start of an integration. The integration was then carried out either until a steady state was closely approached, or until θ_{CO} became equal to $(\theta_{CO})_H$. If the latter condition occurred, then the value of ψ was changed to a value greater than unity (150 for results reported in this study). The integration was then continued either until a steady state was closely approached or until θ_{CO} became equal to $(\theta_{CO})_L$. If the latter situation occurred, then the value of ψ was changed back to unity. The integration was always continued until either stable steady-state or stable cycling behavior was achieved.

Effect of CO Feed Concentration

The experimentally determined effects of feed CO concentration on oscillatory behavior at 393 K are shown in Fig. 6 of Ref. (*1*). The behavior predicted by the model, with $(\theta_{CO})_H = 0.95$ and $(\theta_{CO})_L = 0.1$, is shown in Fig. 5. The predicted oscillations shown in Fig. 5 have many features in common with the corresponding experimental observations shown in Fig. 6 of Ref. (*1*). First, considering an individual oscillation, it is seen that the predicted shape (broad minimum, fast rise to a local maximum, more gradual rise to a global maximum, etc.) is in excellent agreement with the experimental observations. Second, it is seen that the majority of the systematic experimental trends are predicted to occur by the model. The following points of agreement are seen to occur.

1. As the concentration of CO in the feed is decreased the system moves from a low conversion steady state to an oscillatory state. The period of the oscillation is initially very long, with a broad minimum and a short, steep rise after the local maximum.
2. When the concentration of CO in the feed is decreased further, the breadth of the minimum decreases rapidly causing the period of the oscillation to decrease. The slope of the rise after the local maximum decreases, and the amount of time spent in the high conversion portion of the oscillation increases.
3. The period of the oscillation goes through a minimum as the feed CO concentration is decreased due to the compensating effects of the decrease in the breadth of the minimum and the increase in the length of the rise portion after the local maximum.
4. As the feed CO concentration is further decreased, the period of the oscillation becomes extremely long, with the main portion of the oscillation consisting of a long, slow rise to a global maximum in the CO_2 effluent concentration.
5. Finally the system passes to, and remains at, a high conversion steady state for very low values of the percentage CO in the feed.

One point that should be emphasized is the correct variation of the period of the oscillation due to the variation in feed CO concentration. If CO feed compositions are chosen between 0.37 and 0.365% (or between 0.27 and 0.28%) it is possible to obtain extremely long period oscillations, and in fact the period becomes infinitely long just prior to the transition to the stable steady state. This predicted behavior, and the fact that it is in agreement with the experimental data, is important because prior models (*3, 5, 11*) which have relied on the occurrence of a Hopf bifurcation to produce oscillations do not predict this behavior. When a system moves from stable to oscillatory behavior via a Hopf bifurcation, the first oscillations to occur are small amplitude, harmonic oscillations with a period approaching zero near the bifurcation point.

Although the model predictions are in qualitative agreement with all of the experimental observations, two areas of quantitative disagreement are apparent: one, the predicted variation of the amplitudes of the oscillations does not agree with the experimental observations, and two, the CO feed concentrations at which transitions occur from stable states to oscillatory behavior are not in total agreement. One possible cause for these deviations is the isothermal assumption inherent in the model; i.e., it is assumed that the temperature of the metal crystallites is equal to the bulk temperature. Variations in metal crystallite temperature during an oscillation will certainly influence the amplitude of the oscillation. The mismatch in the transitions from steady-state to oscillatory behavior is possibly due to the fact that the model predicts oscillations outside of the gaps shown in Fig. 4. This interesting observation can be seen by comparing the values of the CO feed concentrations used in Fig. 5 with the steady-state results presented in Fig. 3. It is seen

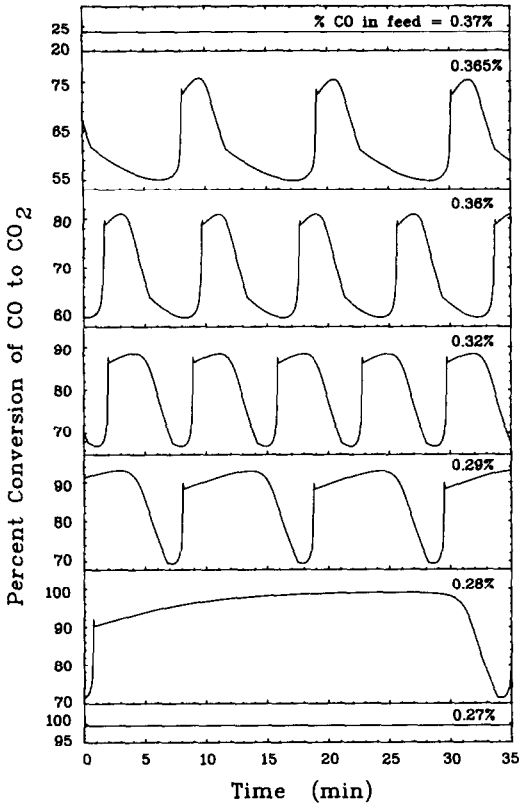

FIG. 5. Predicted effect of feed CO concentration on CO_2 oscillations.

that, while the oscillations for $0.28 \leq \%CO \leq 0.36$ are clearly in the gap region in Fig. 3, the oscillation at 0.365% CO is occurring in a region where a stable steady state exists. The stability of the oscillation is dependent on whether its trajectory passes through the region of attraction of the stable steady state. This of course is very strongly affected by the choice of $(\theta_{CO})_H$. The coexistence of oscillations with a stable steady state has been reported for hydrogen oxidation (*21*), but to our knowledge this has not been reported for CO oxidation. This phenomenon was not observed during the study reported in Ref. (*1*) because the operating parameters were varied only in a single direction. Additional experimental work is clearly needed in order to determine if this predicted phenomenon does indeed occur. It was primarily due to this phenomenon that no attempt was made to obtain closer agreement between the predicted regions of oscillatory behavior from the steady-state calculations and the experimental regions. The model predicts that this phenomenon can also occur in a limited region of CO feed concentrations when the oscillatory behavior passes to the high conversion steady state.

Effect of Total Molar Feed Rate

In Fig. 6 are shown the model predictions for the effect of variation of the total molar flow rate on the oscillatory behavior. It is seen that varying the total molar flow rate has much the same effect as varying the CO concentration in the feed. A comparison of Fig. 6 with Fig. 5 of Ref. (*1*) illustrates that, with the exception of the oscillation amplitude, the model correctly predicts all of the systematic trends that were observed experimentally. The effect of increasing the flow rate is very similar to that for increas-

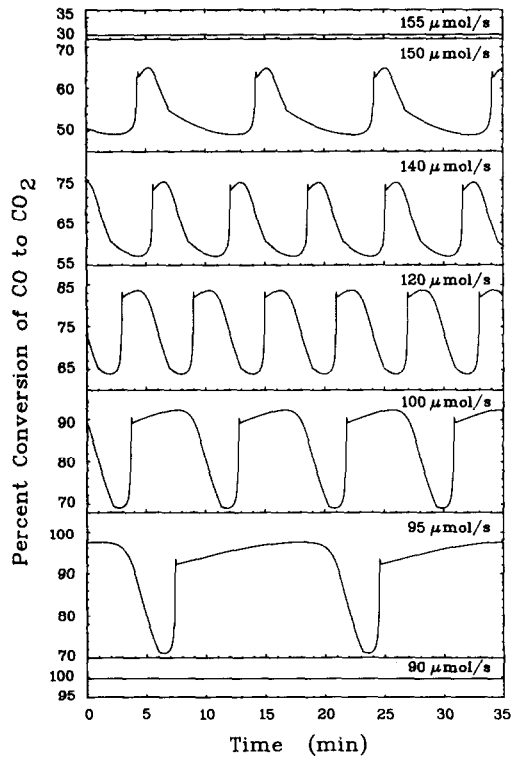

FIG. 6. Predicted effect of total molar feed rate on CO_2 oscillations.

ing the CO concentration in the feed because both cases affect the molar flow of CO into the reactor. The molar flow of CO has a major effect on the period of the oscillations because the period of the oscillation is largely determined by the time required for θ_{CO} to vary between $(\theta_{CO})_L$ and $(\theta_{CO})_H$, or vice versa. During much of an oscillation a very sensitive balance exists between the rates of adsorption and the surface reaction rate; thus the accumulation or removal of CO can require much more time than that required just for adsorption in the absence of reaction, or reaction in the absence of adsorption.

For example, for any of the conditions used in Figs. 5 and 6, less than 0.4 s are needed to produce $\theta_{CO} = 0.95$ from an initially clean surface with $X = 1$ maintained during the adsorption, and with both Y and θ_O kept at zero throughout. Thus, CO adsorption is not a limiting step by itself. If θ_{CO} and θ_O are both initially set to 0.5, then less than 5 s are required to reduce θ_{CO} to 0.1, with an inert feed steam ($F_{CO} = F_{O_2} = 0$) passing through the reactor. Thus the reaction rate is not limiting by itself. However, if the surface is in phase 1 ($\psi = 1$), more than 800 s are required to produce $\theta_0 = 0.95$ from an initially clean surface with a pure oxygen feed to the system, while less than 6 s are required to produce $\theta_0 = 0.95$ when $\psi = 150$.

For the oscillations shown in Figs. 5 and 6, phase 1 is present during that portion of the oscillation beginning at the local maximum, passing through the rise to the global maximum, and ending at the inflection point during the drop to the minimum. During this part of the oscillation, which can last from several to more than 30 min, CO is accumulating on the catalyst surface. The time necessary for the θ_{CO} to reach $(\theta_{CO})_H$ is not solely dependent on the rate of adsorption of the CO, but rather it is fixed by the net rate of CO accumulation, which is in turn fixed by the rate of oxygen adsorption with subsequent reaction. During the remainder of the oscillation, the portion stretching from the inflection point, through the global minimum, and ending at the local maximum, phase 2 is present. From the preceding calculations, the time to pass through this portion of the oscillation, which can be from less than a minute to more than 10 min, cannot be attributed to the limitation of a single elementary step. Thus, the breadth of the minimum region is due to a very sensitive balance between the adsorption and the reaction steps, since in isolation the time scale for any of the individual steps is at least an order of magnitude smaller than that for the oscillation.

Effect of Bulk Temperature

Shown in Fig. 7 are the predicted effects on the oscillatory behavior due to the variation of the bulk temperature of the reactor. A comparison of Fig. 7 with Fig. 3 in Ref. (*1*) shows that all of the systematic trends, including the variation of amplitude, are correctly predicted by the model. The only

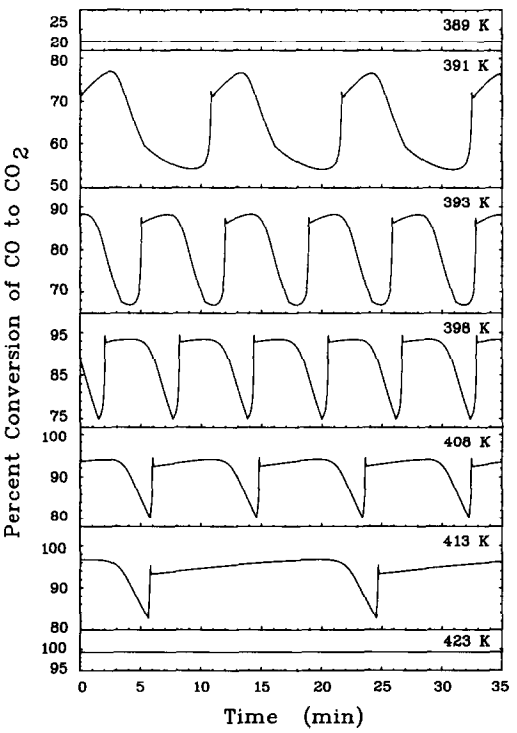

FIG. 7. Predicted effect of reactor temperature on CO_2 oscillations.

phenomenon not predicted by the model is the occurrence of chaos in the intermediate temperature region. To predict chaos it is necessary for a second oscillator to exist, possibly through the action of one of the previously mentioned hypotheses, such as surface temperature variation. The prediction of chaos by this model through the use of an additional hypothesis is currently being investigated.

Before the model predictions shown in Fig. 7 could be determined, it was necessary to specify the temperature dependence of the various parameters. It was found that the temperature ($\simeq$390 K) of the transition from oscillatory to stable low conversion steady-state behavior was affected mainly by the value of the activation energy for CO desorption. The high temperature ($\simeq$418 K) transition point was affected mainly by the value of the activation energy for the surface reaction. Since these two effects are largely decoupled in the model it is always possible to obtain excellent agreement between the predicted and the experimental temperature regions for oscillatory behavior. However, it was found that if $(\theta_{CO})_H$ was maintained at 0.95 then the minimum portion of the oscillation became broader (instead of sharper) as the temperature was increased. The sharp, high temperature oscillations shown in Fig. 7 were obtained by assuming that the surface phase change process is very slightly activated with E/R =750 K. This results in $(\theta_{CO})_H$ decreasing from 0.95 at 393 K to 0.87 at 413 K. It was not necessary to include an activation energy for $(\theta_{CO})_L$ since this parameter could be varied over a wide range without having a significant effect on the model predictions. Alternatively, the sharpening of the minimum region of the oscillations can also be obtained by assuming that the adsorption of oxygen on phase 1 is slightly activated. However, this assumption was not used in the predictions shown in Fig. 7.

Effect of Diluents

In Figs. 5 to 7, the model predictions with respect to the oscillations of the CO_2 leaving the reactor have been examined in detail. To further validate the model, the predictions with respect to the exit CO concentrations have also been calculated, and are shown in Fig. 8. In this figure the effect of changing the percentage of oxygen in the reactor feed (CO feed concentration is constant) is examined. This figure should be compared to Fig. 8 of Ref. (*1*), where analogous experimental results are presented. With respect to an individual CO oscillation, it is seen that all of the basic features are predicted by the model, namely; a rapid rise to a maximum, followed by a slow decrease, with a subsequent rapid (almost instantaneous) decrease to almost no CO in the reactor effluent (100% conversion). The prediction, in agreement with the experimental observations, that the CO concentration should remain near zero for a relatively long period of time during each oscillation is particularly important. It has been found, when examining other models, that this is one of the most difficult regions in which to obtain agreement with the experimentally observed CO oscillations. In addition to the agreement obtained with respect to a single oscillation, it is also seen that the model correctly predicts the trends in the variation of the shape of the CO oscillations when the percentage of oxygen in the reactor feed is reduced. This is particularly evi-

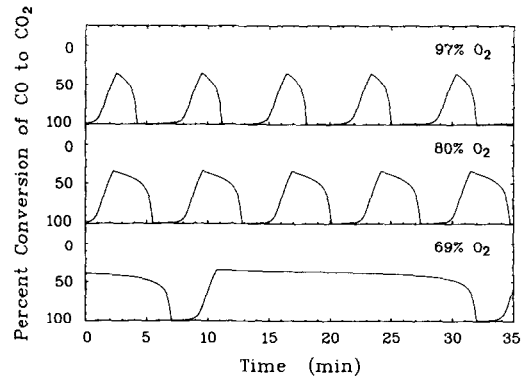

FIG. 8. Predicted effect of diluents on CO oscillations.

dent when comparing the very long period oscillations, i.e., 69% O_2 in Fig. 8 versus 50.1% O_2 in Fig. 8 of Ref. (*1*).

SUMMARY AND CONCLUSIONS

The hypothesis that the adsorption of CO causes portions of a catalyst surface to undergo a reversible phase change has been incorporated into a mathematical model. The predictions of this model have been shown to be in agreement with the steady-state and dynamic behavior previously reported for the oxidation of CO on a supported catalyst (*1*). This model correctly predicts the details of the shapes and frequencies of the CO and CO_2 oscillations over a wide range of operating parameters. To our knowledge, this is the first time that such detailed agreement has been obtained between model predictions and experimental observations for the oscillatory behavior of catalytic CO oxidation. It has been shown that the period of an oscillation can be divided into two parts, namely, a region where oxygen adsorption limitations are important, and a region where a sensitive balance exists between adsorption and reaction steps.

This model cannot predict the occurrence of chaotic behavior; however, as shown previously (*22*), the coupling of two oscillators in a reaction system can give rise to this type of behavior. We believe that the incorporation of surface temperature effects in this model will result in the prediction of chaotic behavior. Work is currently proceeding in this direction.

The excellent model–experimental agreement obtained in this study does not guarantee that the surface phase change hypothesis is correct; however, alternate hypotheses should only be considered after they have been shown to be capable of producing the high degree of experimental–model agreement demonstrated in this study. If two or more hypotheses are capable of producing similar agreement, then the competing mathematical models should be used to design incisive experiments so as to critically discriminate among the various hypotheses.

APPENDIX: NOMENCLATURE

a_m	Total surface area of the supported catalyst, 1 m^2
a_s	Total surface area of the support, 1700 m^2
E_{-1}/R	CO desorption activation energy for catalyst, 9000 K
E_3/R	Surface reaction activation energy, 8000 K
E_{-4}/R	CO_2 desorption activation energy from support, 10,000 K
[CO]	Reactor, and exit, CO concentration, mol/m^3
$[CO]_0$	Feed CO concentration, $F_{CO}P/RT$, mol/m^3
$[CO_2]$	Reactor, and exit, CO_2 concentration, mol/m^3
F_{CO}	Fraction CO in feed, 0.0032 unless otherwise indicated
F_{O_2}	Fraction O_2 in feed, $F_{O_2} = 1 - F_{CO}/0.11$, unless otherwise indicated
k_1	CO adsorption rate constant
k_{-1}	CO desorption preexponential factor, 4×10^9 $mol/m^3 \cdot s$
$k_{2,1}$	O_2 adsorption rate constant on phase 1
$k_{2,2}$	O_2 adsorption rate constant on phase 2
k_3	Surface reaction rate constant, 5.8×10^{13} s^{-1} m^{-1}
k_4	CO_2 adsorption rate constant
k_{-4}	CO_2 desorption preexponential factor, 2.5×10^9 $mol/m^3 \cdot s$
K_1	Dimensionless CO adsorption rate constant
K_{-1}	Dimensionless CO desorption rate constant
K_2	Dimensionless O_2 adsorption rate constant
K_3	Dimensionless surface reaction rate constant
K_4	Dimensionless CO_2 adsorption rate constant
K_{-4}	Dimensionless CO_2 desorption rate constant

L_m Adsorption capacity of the metal surface, 2×10^{-5} mol/m^2

L_s CO_2 adsorption capacity of the support, 1.2×10^{-6} mol/m^2

$[O_2]$ Reactor, and exit, O_2 concentration, mol/m^3

$[O_2]_0$ Feed O_2 concentration, $F_{O_2}P/RT$, mol/m^3

P Reactor pressure, 0.101 MPa absolute

Q_n Ratio of exit to feed volumetric flow rates

Q_0 Feed volumetric flow rate at reactor conditions, based on a total molar flow rate of 108 μmol/s unless otherwise indicated

R Gas constant, 8.3144 Pa · m^3/mol · K

S_{CO} CO sticking probability on catalyst, 2×10^{-5}

S_{CO_2} CO_2 sticking probability on support, 6×10^{-8}

S_{O_2} O_2 sticking probability on catalyst, 6×10^{-11}

t Time, s

T Reactor temperature, 393 K unless otherwise indicated

V Reactor volume, 2.5×10^{-4} m^3

X Dimensionless reactor CO concentration, $[CO]/[CO]_0$

Y Dimensionless reactor O_2 concentration, $[O_2]/[O_2]_0$

Z Dimensionless reactor CO_2 concentration, $[CO_2]/[CO]_0$

Greek Symbols

α_m Ratio of bulk volume to metal surface capacitances

α_s Ratio of bulk volume to support surface capacitances

θ_{CO} Fractional CO surface coverage on the metal surface

$(\theta_{CO})_H$ High critical value of θ_{CO} at which the phase 1 to 2 transformation occurs (0.95 at 393 K used herein)

$(\theta_{CO})_L$ Low critical value of θ_{CO} at which the phase 2 to 1 transformation occurs (0.1 used in this study)

θ_0 Fractional oxygen surface coverage on the metal surface

τ Dimensionless time based on the reactor residence time

ϕ_{CO_2} Fractional CO_2 surface coverage on the support surface

ψ Multiplier for S_{O_2}, 1 for surface phase 1, 150 for surface phase 2

ACKNOWLEDGMENTS

This work has been supported by the Natural Sciences and Engineering Research Council of Canada.

REFERENCES

1. Lynch, D. T., and Wanke, S. E., *J. Catal.* **88,** 345 (1984).
2. Belyaev, V. D., Slin'ko, M. M., Slin'ko, M. G., and Timoshenko, V. I., *Dokl. Akad. Nauk SSSR* **214,** 1098 (1974).
3. Pikios, C., and Luss, D., *Chem. Eng. Sci.* **32,** 191 (1977).
4. Hugo, P., and Jakubith, M., *Chem. Ing. Tech.* **44,** 383 (1972).
5. Dagonnier, R., and Nuyts, J., *J. Chem. Phys.* **65,** 2061 (1976).
6. Dagonnier, R., Dumont, M., and Nuyts, J., *J. Catal.* **66,** 130 (1980).
7. Jensen, K. F., and Ray, W. H., *Chem. Eng. Sci.* **37,** 1387 (1982).
8. Lynch, D. T., and Wanke, S. E., *in* "Proceedings, 32nd CSChE Conference, Vancouver, 1982," Vol. 2, p. 852.
9. Eigenberger, G., *Chem. Eng. Sci.* **33,** 1263 (1978).
10. Mukesh, D., Cutlip, M. C., Goodman, M., Kenney, C. N., and Morton, W., *Chem. Eng. Sci.* **37,** 1807 (1982).
11. Morton, W., and Goodman, M. G., *Trans. Inst. Chem. Eng.* **59,** 253 (1981).
12. Sales, B. C., Turner, J. E., and Maple, M. B., *Surf. Sci.* **114,** 381 (1982).
13. Ertl, G., Norton, P. R., and Rüstig, J., *Phys. Rev. Lett.* **49,** 177 (1982).
14. Lynch, D. T., and Wanke, S. E., *J. Catal.* **88,** 333 (1984).
15. Behm, R. J., Thiel, P. A., Norton, P. R., and Ertl, G., *J. Chem. Phys.* **78,** 7437 (1983).
16. Thiel, P. A., Behm, R. J., Norton, P. R., and Ertl, G., *J. Chem. Phys.* **78,** 7448 (1983).
17. Barteau, M. A., Ko, E. I., and Madix, R. J., *Surf. Sci.* **102,** 99 (1981).
18. Norton, P. R., Davies, J. A., Creber, D. K., Sit-

ter, C. W., and Jackman, T. E., *Surf. Sci.* **108,** 205 (1981).

19. Pirug, G., Broden, G., and Bonzel, H. P., *in* "Proceedings of the Seventh International Vacuum Congress and the Third International Conference on Solid Surfaces, Vienna, 1977," p. 907.

20. Fehlberg, E., *Computing* **6,** 61 (1970).

21. Rajagopalan, K., and Luss, D., *J. Catal.* **61,** 289 (1980).

22. Lynch, D. T., Rogers, T. D., and Wanke, S. E., *Math. Model.* **3,** 103 (1982).